JOURNAL OF Materials CHEMISTRY

Second-order non-linear optical properties of 'bent' ferrocenyl derivatives

José A. Campo,[a] Mercedes Cano,*[a] José V. Heras,[a] Carolina López-Garabito,[a] Elena Pinilla,[a,b] Rosario Torres,[b] Gema Rojo[c] and Fernando Agulló-López*[c]

[a]*Departamento de Química Inorgánica I, Facultad de Ciencias Químicas, Universidad Complutense, 28040 Madrid, Spain*
[b]*Laboratorio de Difracción de Rayos-X, Facultad de Ciencias Químicas, Universidad Complutense, 28040 Madrid, Spain*
[c]*Departamento de Física de Materiales, Facultad de Ciencias, Universidad Autónoma de Madrid, 28049 Madrid, Spain*

Received 16th November 1998, Accepted 22nd December 1998

The organometallic compounds [4-$O_2NC_6H_3$(2-CH_3)N=NC_6H_3(5′-CH_3)-2′-(η^5-C_5H_4)Fe(η^5-C_5H_5)] **1** and [Mo(Cl)(Tp^{An})(NO){NHC_6H_3(3-CH_3)[N=NC_6H_3(5-CH_3)-2-(η^5-C_5H_4)Fe(η^5-C_5H_5)]-4}] **2** {Tp^{An} = hydrotris[3-(*p*-methoxyphenyl)pyrazol-1-yl]borate} have been synthesized, characterized and their second-order non-linear optical (NLO) properties studied. In both cases the location of the ferrocenyl donor group at the *ortho* position of the aryl group with respect to the N=N group breaks the 'molecular linearity' defined by the bridging axis between the donor and acceptor groups. The crystal structure of **1** has been determined to be non-centrosymmetric, by contrast to the centrosymmetric related 'linear' compound [4-$O_2NC_6H_3$(2-CH_3)N=NC_6H_4-4′-(η^5-C_5H_4)Fe(η^5-C_5H_5)] having the ferrocenyl group at the *para* position of the aryl group. The three non-zero components of the second-harmonic susceptibility $\chi_{ij}^{(2)}$ ($2\omega;\omega,\omega$) tensor have been determined for poled poly(methyl methacrylate) films containing compounds **1** and **2**; $\chi_{31}^{(2)} > \chi_{33}^{(2)}$, suggesting a tilted (non-parallel) optical transition moment in relation to the permanent dipole moment. This also may account for the breaking of Kleinman's symmetry under near-resonant conditions, *i.e.* $\chi_{15}^{(2)} \neq \chi_{31}^{(2)}$. Moreover, by comparing the results with those of related compounds having the ferrocenyl group in the *para* position of the aryl group, it has been concluded that molecular 'bending' strongly reduces the second-order NLO response, but it maintains strong off-diagonal ($\chi_{31}^{(2)}$) components of the $\chi_{ij}^{(2)}$ tensor.

Introduction

The study of molecular materials with second-order non-linear optical (NLO) properties has been the subject of intense interest in recent years because of their potential applications in optoelectronics technology. Most of the work has been focused on organic molecules because of the promise of large NLO responses, fast response times and convenient optimization routes through molecular engineering.[1–7] However, since the first report in 1987 about the high second-harmonic generation (SHG) yield of an organometallic compound,[8] the research on this type of compounds for NLO has experienced a fast rise.[9,10]

It has been established that a main route for the design of efficient second-order NLO molecules involves electron-donor and electron-acceptor groups bridged by a π-conjugated system and possessing low-lying charge-transfer excited states.[1,2,11,12] Organometallics having a metal centre bonded to a π-conjugated ligand system should display large molecular hyperpolarizabilities because of the charge-transfer density between the metal atom and the conjugated ligand. Unfortunately, most of the NLO results on organometallic compounds using the Kurtz powder test have yielded low or no response. This fact has been attributed to the inability to produce non-centrosymmetric media.[10]

In a previous paper[13] the second-order NLO response of the molecules [4-$O_2NC_6H_4CH$=CHC_6H_4-4′-(η^5-C_5H_4)Fe(η^5-C_5H_5)] and [Mo(Cl)(Tp^{An})(NO){HNC_6H_3(3-R)[Z=ZC_6H_3(3-R′)-4-(η^5-C_5H_4)Fe(η^5-C_5H_5)]-4}] {Z = N, R = R′ = H or CH_3; Z = N, R = CH_3, R′ = H; Z = CH, R = R′ = H; Tp^{An} = hydrotris[3-(*p*-methoxyphenyl)pyrazol-1-yl]borate} has been determined. In these systems an electron-donor metal fragment (ferrocenyl group) was strongly coupled to an electron-acceptor group of the type NO_2 or [Mo(Cl)(Tp^{An})(NO)] through a π system. The role of diverse π-bridging structures including different lengths, substituents and polarizable groups, as well as the influence of the acceptor group NO_2 *vs.* [Mo(Cl)(Tp^{An})(NO)], has been evaluated. In addition our experimental results suggested that the two (transition and permanent) dipole moments are not aligned but tilted with regard to each other. Since the permanent dipole moment is reasonably associated with the molecular axis connecting the donor and acceptor groups, the transition dipole moment should have a component along the transverse direction.[13]

The final goal of our research is to prepare organometallic compounds favouring non-centrosymmetric crystalline structures, but keeping high enough values for the quadratic hyperpolarizability β. To that end the role of molecular geometry and particularly molecular linearity has been now specifically addressed.

Here we describe the preparation, characterization and the second-order NLO properties of the new complexes [4-$O_2NC_6H_3$(2-CH_3)N=NC_6H_3(5′-CH_3)-2′-(η^5-C_5H_4)Fe(η^5-C_5H_5)] **1** and [Mo(Cl)(Tp^{An})(NO){NHC_6H_3(3-CH_3)-[N=NC_6H_3(5-CH_3)-2-(η^5-C_5H_4)Fe(η^5-C_5H_5)]-4}] **2**, whose molecular structures are illustrated in Fig. 1. These complexes were designed to have the ferrocenyl group at the *ortho* position of the aryl group with regard to the bridging charge-transfer axis, in contrast to those previously having this group in the *para* position.[13] Then, the effect of breaking the 'molecular linearity' on the SHG responses has been investigated by comparing the results for both types of compounds with those previously obtained for the 'linear' related complexes.[13] The crystalline structure of **1** has also been solved by X-ray diffraction, showing a non-centrosymmetric space group, thus a NLO response should be expected.

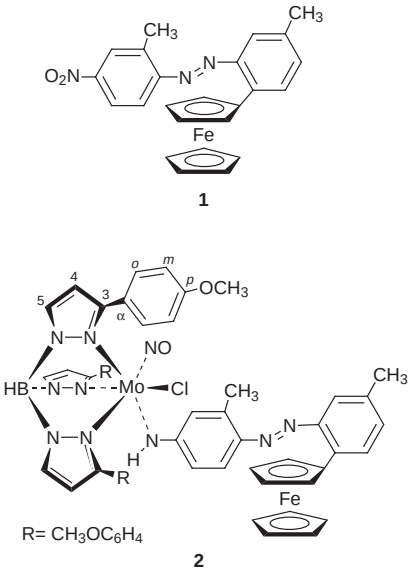

Fig. 1 Molecular structure for compounds **1** and **2**.

Measurements of SHG have been carried out on spin-coated poly(methyl methacrylate) (PMMA) host films containing compounds **1** and **2**. Molecular ordering was achieved by the corona poling procedure.[14] In this way, the data reflect the molecular NLO behavior, at variance with those obtained by the common Kurtz powder method, where crystal symmetry restrictions are often dominant. Moreover, thin films offer a most promising route for technological applications.

Results and discussion

Synthesis and spectroscopic characterization

The preparation of the 'bent' molecule $[4\text{-}O_2NC_6H_3\text{-}(2\text{-}CH_3)N{=}NC_6H_3(5'\text{-}CH_3)\text{-}2'\text{-}(\eta^5\text{-}C_5H_4)Fe(\eta^5\text{-}C_5H_5)]$ **1** (Scheme 1) has been performed by a Mills condensation reaction (step f) between both nitroso and amine groups from 5-nitro-2-nitrosotoluene **D** and 2-ferrocenyl-5-methylaniline **B**, which in turn have been obtained by oxidation of 2-methyl-4-nitroaniline **C** (step e) and ferrocenium arylation (steps a–c) followed by a reduction of the nitro group to amine (step d) respectively. This procedure is analogous to that used for the synthesis of related complexes.[15]

The bimetallic 'bent' molecule $[Mo(Cl)(Tp^{An})(NO)\text{-}\{NHC_6H_3(3\text{-}CH_3)[N{=}NC_6H_3(5\text{-}CH_3)\text{-}2\text{-}(\eta^5\text{-}C_5H_4)Fe(\eta^5\text{-}C_5H_5)]\text{-}4\}]$ **2** has been synthesized by reaction of $[Mo(Cl)_2\text{-}(Tp^{An})(NO)]$ with the ligand $[4\text{-}H_2NC_6H_3(2\text{-}CH_3)N{=}NC_6H_3\text{-}(5'\text{-}CH_3)\text{-}2'\text{-}(\eta^5\text{-}C_5H_4)Fe(\eta^5\text{-}C_5H_5)]$ **E** obtained by reduction of **1** (Scheme 1, steps g and h). The new compounds have been fully characterized by spectroscopic and analytical techniques. The data of the new intermediates **A**, **B** and **E** are given in the Experimental section. Table 1 lists the analytical and spectroscopic data of **1** and **2**. Both complexes show intense molecular-ion peaks in their FAB mass spectra along with varying numbers of fragments.

The IR spectra of complexes **1** and **2** exhibit absorptions due to the different groups. For both cases an absorption band at *ca.* 900 cm^{-1} characteristic of monoaryl-substituted ferrocenyl groups is clearly observed.[15,16] In addition the bands from the acceptor fragments, NO_2 or $[Mo(Cl)(Tp^{An})(NO)]$ for **1** and **2** respectively (Table 1), do not show significant variations with respect to the related *para*-ferrocenyl compounds $[4\text{-}O_2NC_6H_3(2\text{-}CH_3)N{=}NC_6H_3(3'\text{-}CH_3)\text{-}4'\text{-}(\eta^5\text{-}C_5H_4)Fe(\eta^5\text{-}C_5H_5)]$ **1**′ and $[Mo(Cl)(Tp^{An})(NO)\{NHC_6H_3(3\text{-}CH_3)[N{=}NC_6H_3(3\text{-}CH_3)\text{-}4\text{-}(\eta^5\text{-}C_5H_4)Fe(\eta^5\text{-}C_5H_5)]\text{-}4\}]$ **2**′. So, the $\nu(NO_2)$ (asymmetric and symmetric) absorption bands

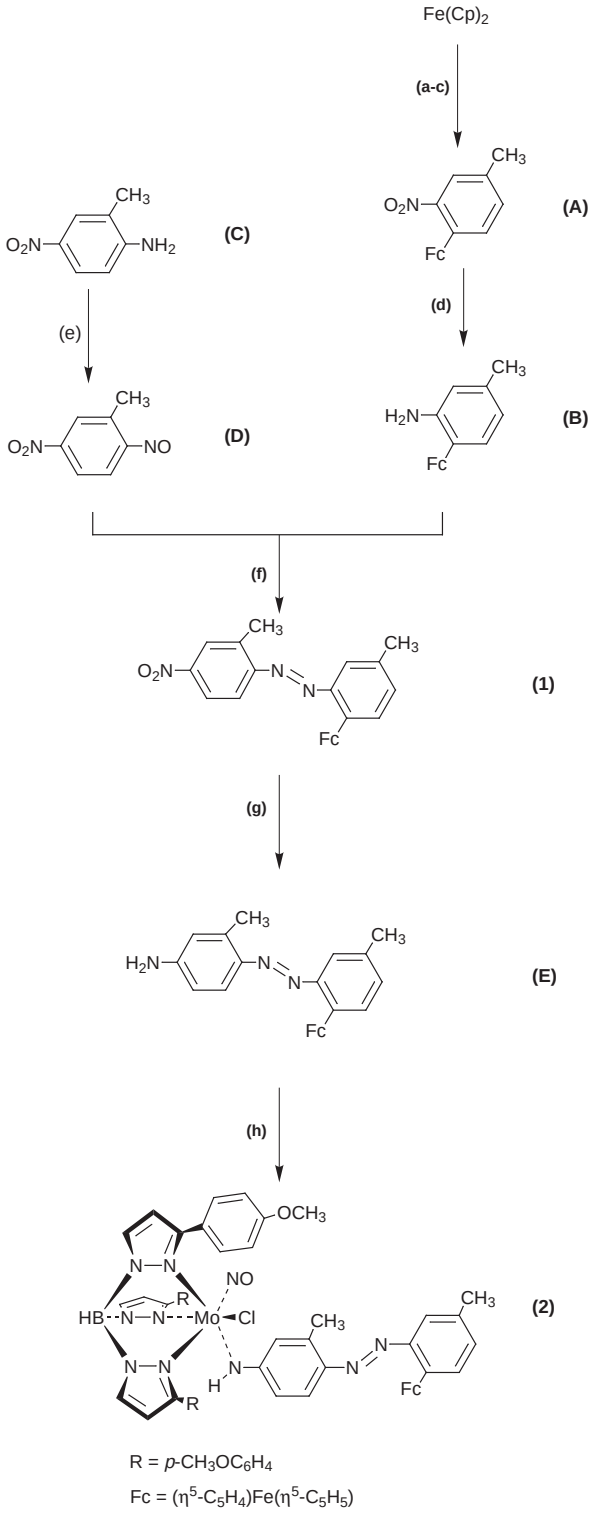

Scheme 1

appear at 1525 and 1343 cm^{-1} for **1** and at 1520 and 1345 cm^{-1} for **1**′.[15] The same behavior is also observed for the ν(NO) and ν(NH) bands, which are shown at 1675 and 3283 cm^{-1} for **2** and at 1675 and 3281 cm^{-1} for **2**′.[13] On the other hand, the **ν**(BH) stretch in **2** is clearly observed at 2490 cm^{-1}.

The ^1H and ^{13}C NMR spectra of the new complexes **1** and **2** (Table 1) contain signals attributable to all protons and carbons of the molecules. The ^1H NMR spectra have been fully assigned by homonuclear decoupling techniques. In the spectra of **2** three signals for each hydrogen or carbon atoms of the Tp^{An} ligand are observed, this fact being consistent with an inequivalence of the three pyrazolyl groups and therefore

Table 1 Analytical and spectroscopic data of compounds **1** and **2**

		1	**2**
Analyses (%)[a]	C	65.42 (65.61)	58.53 (58.89)
	H	4.91 (4.83)	4.82 (4.59)
	N	9.50 (9.57)	12.23 (12.10)
FAB^+	m/z	439 (M^+)	1102 (M^+)
			1067 ($M-Cl^+$)
IR (KBr, cm^{-1})	$\nu(NO_2)$	1525, 1343	
	$\pi(CH)$	895	893
	$\nu(NH)$		3283
	$\nu(BH)$		2490
	$\nu(NO)$		1675
^1H NMR (δ; J/Hz)[b]	NH		12.61 (s, 1 H)
	H4		6.25 (d, $^3J=2.1$, 1H), 6.37 (d, $^3J=2.1$, 2H)
	H5		7.85 (d, $^3J=2.1$, 1H), 7.84 (d, $^3J=2.1$, 1H) 7.83 (d, $^3J=2.1$, 1H)
	H_o		7.89 (d, $^3J=8.7$, 2H), 7.58 (d, $^3J=8.7$, 2H) 6.97 (d, $^3J=8.7$, 2H)
	H_m		6.98 (d, $^3J=8.7$, 2H), 6.71 (d, $^3J=8.7$, 2H), 6.38 (d, $^3J=8.7$, 2H)
	CH_3O		3.87 (s, 3H), 3.57 (s, 3H), 3.40 (s, 3H)
	C_6H_3	8.25 (d, $^4J=2.1$, 1H), 7.66 (d, $^3J=8.8$, 1H), 8.15 (dd, $^3J=8.8$, $^4J=2.1$, 1H)	7.60 (d, $^3J=8.7$, 1H), 7.32 (s, 1H), 7.16 (dd, $^3J=8.7$, $^4J=$ 1.5, 1H)
	C_6H_3	7.72 (d, $^3J=8.0$, 1H), 7.39 (s, 1H), 7.28 (d, $^3J=8.0$, 1H)	7.33 (d, $^3J=8.7$, 1H), 6.23 (d, $^4J=1.5$, 1H), 6.31 (dd, $^3J=8.7$, $^4J=1.5$, 1H)
	CH_3	2.85 (s, 3H), 2.40 (s, 3H)	2.55 (s, 3H), 2.39 (s, 3H)
	C_5H_4	4.76 (t, $^3J=1.8$, 2H), 4.41 (t, $^3J=1.8$, 2H)	4.80 (br s, 1H), 4.75 (br s, 1H), 4.40 (br s, 2H)
	C_5H_5	4.06 (s, 5H)	4.04 (s, 5H)
^{13}C NMR (δ)[b]	C3		157.8, 157.2, 157.0
	C4		108.5, 108.1, 107.7
	C5		137.1, 136.8, 136.3
	C_α		125.9, 124.2, 123.9
	C_o		131.6, 131.0, 130.6
	C_m		113.4, 112.8
	C_p		160.1, 159.5, 159.0
	CH_3O		55.1, 54.7
	C_6H_3	154.2, 150.0, 148.1, 139.0, 137.5, 136.2, 132.4, 130.2, 126.4, 122.0, 116.9, 116.0	159.5, 150.5, 148.1, 138.9, 135.8, 130.9, 129.7, 123.7, 120.4, 116.2, 116.0
	CH_3	21.8, 17.8	20.9, 17.5
	C_5H_4	77.1, 70.8, 69.3	82.8, 70.7, 70.4, 69.0, 68.8
	C_5H_5	69.7	69.5

[a] Calculated in parentheses. [b] In $CDCl_3$ solution at room temperature; s = singlet, d = doublet, dd = doublet of doublets, t = triplet, br s = broad signal.

with the proposed structure. The signals from the aryl and methyl groups in the aza bridges are as expected. On the other hand, complex **1** shows the usual three proton signals (ratio 2:2:5) attributable to the monosubstituted ferrocenyl moiety,[15,17–19] whilst **2** shows a more complex pattern (ratio 1:1:2:5). The signals of the C_5H_4 protons for both compounds appear at lower field than the C_5H_5 singlet, showing that all four ring protons are deshielded by the aryl ring substituent.

X-Ray study of complex 1

An X-ray crystallographic study of compound **1** was carried out. Compound **1** crystallizes in the non-centrosymmetric orthorhombic $Pna2_1$ space group, with two independent molecules (A and B) in the asymmetric unit, which do not show significant differences in bonding parameters. However, slight differences are observed in some dihedral angles.[20] Fig. 2 shows an ORTEP[21] perspective of one of the two molecules (molecule A), with the atomic numbering scheme. Fig. 3 shows the packing arrangement viewed down the x axis. Selected bond distances and angles are listed in Table 2.

The molecule can be described in terms of a planar NO_2 group (acceptor), a ferrocenyl group (donor) having parallel virtually eclipsed cyclopentadienyl rings and a diarylazo group bridging both donor and acceptor groups.

As has been mentioned, the two cyclopentadienyl rings are practically parallel in the two molecules, within the experimental error, with a dihedral angle of 1(1)°. However, they are almost eclipsed with a rotation angle of 12(2) and 6(2)° for molecules A and B respectively.

As expected the ferrocenyl fragment is located in the *ortho* position of the NO_2-free aryl group with respect to the N=N bridge. Thus the molecule is 'bent' in relation to the donor–acceptor charge-transfer axis.

The azo group is *trans* [torsion angle C(12A)–N(1A)–N(2A)–C(17A), 180(2)°] and the phenyl rings are inclined 4(2)° with respect to the azo plane. In turn, the planar fragment NO_2 is rotated 5(1)° in both molecules with respect to its attached phenyl ring and the C_5H_4 fragment is also rotated 37.2(8) and 41.4(8)° with respect to its attached phenyl rings in molecules A and B respectively.

The bond distances and angles (Table 2) are very similar to those found for the related 'linear' (non-bent) compound [4-$O_2NC_6H_3(2\text{-}CH_3)N{=}NC_6H_4\text{-}4'\text{-}(\eta^5\text{-}C_5H_4)Fe(\eta^5\text{-}C_5H_5)$][22] and they fall in the expected range.[22–25]

The most interesting feature revealed by the crystal structure, in view of the NLO properties, is the relative position of the molecules in the unit cell. The latter contains four pairs of molecules, and each two show an opposite head-to-tail arrangement. However, this arrangement does not imply a cancellation of the dipole moments due to the non-linear ('bent') molecular shape (Fig. 3). By contrast, the crystal structure of the related *para*-ferrocenyl compound [4-$O_2NC_6H_3(2\text{-}CH_3)N{=}NC_6H_4\text{-}4'\text{-}(\eta^5\text{-}C_5H_4)Fe(\eta^5\text{-}C_5H_5)$] is centrosymmetric (monoclinic, $P2_1/c$)[22] and therefore all the molecular dipoles are cancelled. These results evidence the

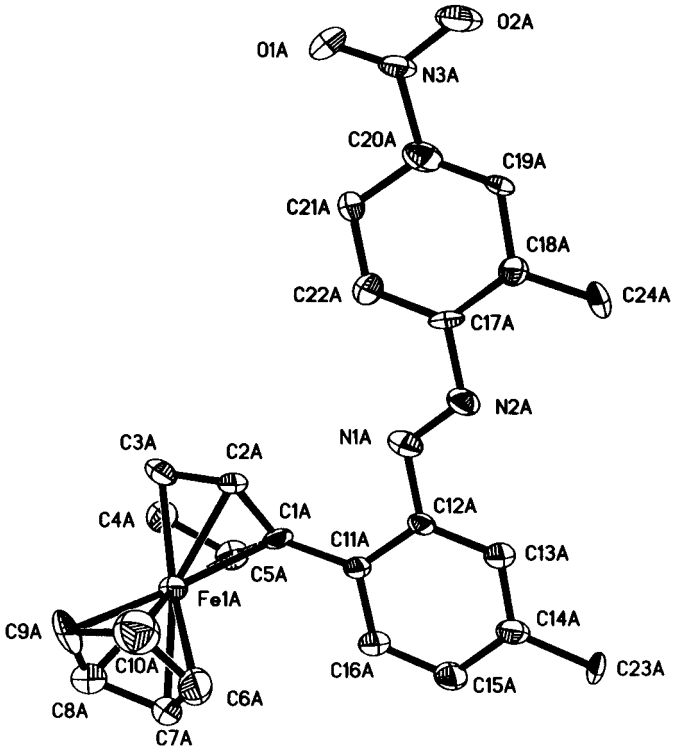

Fig. 2 An ORTEP view of one of the two asymmetry-independent molecules of complex **1** (molecule A) showing the atomic numbering scheme. Hydrogen atoms have been omitted for clarity.

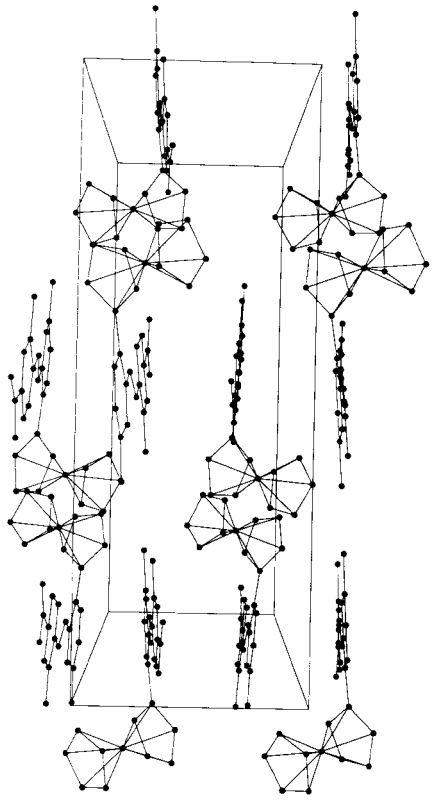

Fig. 3 Packing arrangement of complex **1** viewed down the *x* axis.

effect that the ferrrocenyl position has in breaking the centrosymmetric molecular packing.

Electrochemical studies

The electrochemical behavior of the compounds **1** and **2** has been investigated by cyclic voltammetry in dichloromethane solution and compared with that of the related derivatives **1′** and **2′**.[13] Table 3 lists the voltammetric data. Potentials are referenced to internal ferrocene added at the end of each experiment.

All compounds exhibit a quasireversible oxidation wave ($i_p^c/i_p^a \approx 1$)[26] corresponding to the Fe^{2+}/Fe^{3+} oxidation of the ferrocenyl group. The potentials range from 0.61 to 0.66 V

Table 2 Selected bond distances (Å) and angles (°) for compound **1**

Fe–Cp(1)	1.63(2)	Cp(1)–Fe–Cp(2)	179(1)
Fe–Cp(2)	1.65(2)	C(12A)–N(1A)–N(2A)	117(2)
C(1A)–C(11A)	1.46(3)	N(1A)–N(2A)–C(17A)	117(2)
C(12A)–N(1A)	1.41(3)	C(20A)–N(3A)–O(1A)	124(2)
N(1A)–N(2A)	1.26(3)	C(20A)–N(3A)–O(2A)	112(2)
N(2A)–C(17A)	1.40(2)	O(1A)–N(3A)–O(2A)	124(2)
N(3A)–C(20A)	1.50(4)		
N(3A)–O(1A)	1.19(3)		
N(3A)–O(2A)	1.25(3)		

Cp(1) and Cp(2) indicate the midpoints of the substituted and unsubstituted cyclopentadienyl rings respectively.

Table 3 Electrochemical data of 'bent' derivatives **1** and **2** and related 'linear' compounds **1′** and **2′**[a]

	Ferrocene–ferrocenium		Reductions	
Compound	E_f/V (ΔE_p/mV)	E^b/V	E_f/V (ΔE_p/mV)	E^b/V
1	+0.62 (80)	0.04	−0.70 (65)[c]	−1.28
			−1.00 (110)	−1.58
2	+0.61 (75)	0.03	−0.68 (85)[d]	−1.26
1′[e]	+0.66 (90)	0.08	−0.63 (90)[c]	−1.21
			−0.90 (85)	−1.48
2′[f]	+0.66 (85)	0.08	−0.63 (140)[d]	−1.21
Ferrocene	+0.58 (90)			

[a]All potentials measured relative to Ag–AgCl electrode in dry dichloromethane. [b]Potentials quoted *vs.* ferrocene. [c]Reduction potentials of nitro-azo groups. [d]Reduction potentials of the molybdenum acceptor group. [e]The potentials of this compound have previously been measured relative to SCE[15] (+0.62, −0.77 and −1.03 V). [f]Ref. 13.

(ferrocene, $E_f = 0.58$ V) and they are in agreement with those of previous electrochemical studies on ferrocenyl derivatives.[15,17–19] The E_f values for the iron oxidation increase by *ca.* 40 mV towards more cathodic values on going from 'linear' **1′** or **2′** to 'bent' molecules **1** or **2**. This feature is in accordance with a decrease of the π conjugation of the bridging system, when the ferrocenyl group is moved from the *para* to the *ortho* position at the diarylazo group.

In addition all complexes show cathodic waves attributable to reduction processes from the corresponding acceptor group (Table 3). So the molybdenum derivatives **2** and **2′** showed a quasireversible one-electron molybdenum-based reduction wave, and for the nitro derivatives **1** and **1′** two cathodic, quasireversible and irreversible, waves were observed. A pair of such waves had also been seen for related nitro-azo derivatives and attributed to reduction processes of these groups.[15] The potentials obtained for our compounds are in accord with earlier reports of electrochemical studies on related ferrocenyl derivatives.[15,17–19] The same behavior observed for the oxidation potentials at the ferrocenyl moiety is also found for the reduction processes. So the 'bent' molecules **1** or **2** exhibit more cathodic reduction values than those of related 'linear' ones **1′** or **2′**. This observation is further evidence of the influence of the conjugation size at the bridge.

Another interesting feature emerges on comparing the electrochemical results of the 'bent' molecules **1** and **2** among themselves. So, the oxidation potential of the ferrocenyl moiety is practically not modified and the reduction process is only 20 mV more cathodic in **1** than in **2**. Therefore it can be inferred that the different acceptor groups do not modify the electrochemical properties of the complexes.

Electronic studies

The electronic spectra of complexes **1** and **2** were measured in dichloromethane solution as well as in the spin-coated films prior to poling. Spectra are nearly identical in both cases. This information is very relevant for an adequate discussion of the SHG results.

Peak positions and absorption coefficients are listed in Table 4. For comparative purposes the results of related *para*-ferrocenyl complexes **1′** and **2′** are also included.[13] The spectra are dominated by two bands, one in the ultraviolet region ranging from 340 to 380 nm and the other one in the visible region in the range 480–550 nm. The bands have very high absorption coefficients which provide evidence of extensive charge transfer induced by the optical transition. This feature is important for achieving large hyperpolarizabilities. However, the precise nature of the bands observed is not known.[18]

The spectrum is modified depending upon the position of the ferrocenyl group on the bridge. So, bathochromic shifts are observed on going from the 'bent' to the 'linear' molecules,

Table 4 UV-VIS data of 'bent'derivatives **1** and **2** and related 'linear' compounds **1′** and **2′**[a]

Compound	λ_{max}/nm	ε/dm^3 mol^{-1} cm^{-1}
1	286	13700
	348	15100
	500	
2	342	5400
	484	10500
1′	290	12300
	375	25200
	529	6000
2′	368[b]	1300
	494	17600
	550(sh)	

[a]All spectra recorded in dichloromethane at ambient temperature and concentrations of *ca.* 10^{-4}–10^{-5} M. [b]Ref. 13.

Table 5 Relative change in absorption $\Delta\alpha/\alpha$ and tilting angle ϕ between μ^{01} and $\mu^{(0)}$ for compounds **1** and **2** and the related derivative **2′**

Compound	$\Delta\alpha/\alpha$	ϕ/°
1	−0.035	48
2	0.014	58
2′	−0.014	53

which is in accordance with an increase of the π conjugation in the bridging system.

On the other hand, by comparing the spectra of **1** and **2**, it is seen that the peak position for the low energy charge-transfer band ($\lambda_{max} \approx 500$ nm) is independent of the respective acceptor group, NO_2 or [Mo(Cl)(Tp^{An})(NO)].

The effect of corona poling on the optical absorption spectra of films has been investigated to learn more about the electronic structure. At the peak wavelength corresponding to the lowest energy band ($\lambda_{max} \approx 500$ nm) the measured values of the relative change in the absorption coefficient, $\Delta\alpha/\alpha$, induced by the poling field are given in Table 5. The corresponding value for the *para*-ferrocenyl complex **2′** is also given for comparison. One sees that for the *ortho*-ferrocenyl compounds $\Delta\alpha/\alpha$ is very small. On the other hand, the theoretically expected changes in $\Delta\alpha/\alpha$ as a function of the parameter $p = \mu^{(0)}E/kT$ ($\mu^{(0)}$ being the permanent dipole moment), assuming thermal equilibrium under the field, are given by eqn. (1a)

$$\left(\frac{\Delta\alpha}{\alpha}\right)_{\parallel} = \frac{\alpha(p) - \alpha(0)}{\alpha(0)} = \frac{3}{p}\coth(p) - \frac{e}{p^2} - 1 \qquad (1a)$$

for a transition dipole moment (μ^{01}) parallel to the permanent moment ($\mu^{(0)}$)[27,28] and by eqn. (1b)

$$\left(\frac{\Delta\alpha}{\alpha}\right)_{\perp} = \frac{1}{2} - \frac{3}{2p}\coth(p) + \frac{3}{2p^2} \qquad (1b)$$

for a transition moment, μ^{01}, perpendicular to $\mu^{(0)}$. These dependences with the poling field are shown in Fig. 4. Although the value of p is not known in our experiments, the ratio $\mu_x{}^{01}/\mu_z{}^{01}$, determined from $\Delta\alpha/\alpha$, is essentially independent of p. Therefore, one can obtain meaningful ratios $\mu_x{}^{01}/\mu_z{}^{01}$ assuming any value for p within a reasonable range ($2 < p < 3$). This range is defined by the expected field reached through corona poling (3–4 MV cm^{-1}) and the molecular dipole moments that should be lower than the values measured for the *para*-ferrocenyl compounds.[13] From the ratio $\mu_x{}^{01}/\mu_z{}^{01}$ one can immediately deduce the tilting angle formed by the two,

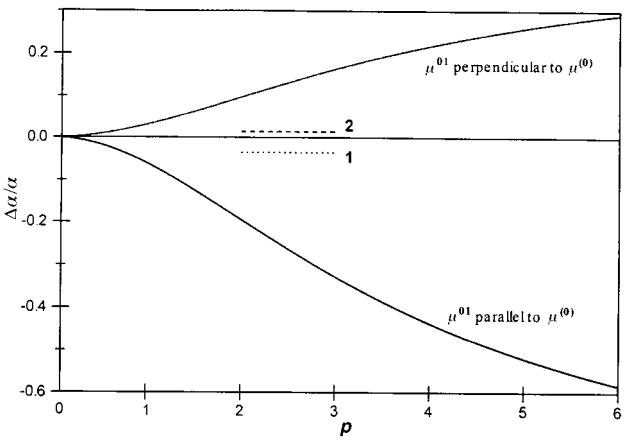

Fig. 4 Theoretical predictions for the relative change in absorption induced by an applied field when μ^{01} is either parallel or perpendicular to $\mu^{(0)}$. The experimental data for compounds **1** and **2** are indicated by short segments.

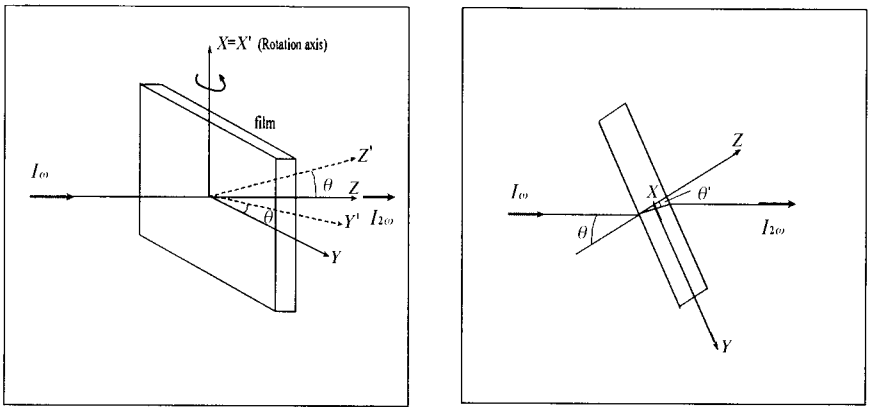

Fig. 5 Experimental geometry: (a) three-dimensional perspective, (b) projection on a plane perpendicular to the rotation (X) axis. X', Y', Z' stand for the film axes and X, Y, Z refer to laboratory axes.

transition and permanent, moments. The calculated values for compounds **1** and **2** are included in Table 5. These angles are higher than those determined for the *para*-ferrocenyl compounds, as observed by comparing **2** and **2′**, also included in Table 5 for comparison. The increase in the tilting angle is, indeed, related to the molecular bending induced by the *ortho* position of the ferrocenyl group in compounds **1** and **2**.

SHG results on films

The listed values were obtained by measuring the SHG yield as a function of the rotation angle θ of the film around the X axis (see Fig. 5). Three different polarization configurations for the fundamental and harmonic beams were used in accordance with Table 6.

The general formula for the SHG emission intensity is[29] eqn. (2),

$$I_{2\omega}(\theta)=\frac{64\pi^3\omega^2{\chi_{\text{eff}}}^2{I_0}^2T}{{n_\omega}^2n_{2\omega}c^3}\,\mathrm{e}^{\frac{-\alpha_{2\omega}L}{2\cos\theta'}}\,\frac{\cosh\left(\frac{\alpha_{2\omega}L}{2\cos\theta'}\right)-\cos\left(\frac{\Delta kL}{\cos\theta'}\right)}{\frac{{\alpha_{2\omega}}^2}{4}+\Delta k^2} \qquad (2)$$

I_0 being the incident fundamental intensity, L the film thickness and T an overall transmission factor accounting for both fundamental and harmonic reflections at the various boundaries. Finally, θ and θ' are the incidence angles for the fundamental wave outside and inside the film, respectively. Other symbols have the usual meaning. Eqn. (2) assumes the validity of the slowly varying amplitude approximation. The effective susceptibility ${\chi_{\text{eff}}}^{(2)}$ depends on the specific polarization configuration as in eqns. (3a)–(3c).[30]

Configuration (1):

$${\chi_{\text{eff}}}^{(2)}=-{\chi_{31}}^{(2)}\sin\theta'=-{\chi_{31}}^{(2)}\frac{\sin\theta}{n_\omega} \qquad (3a)$$

Configuration (2):

$${\chi_{\text{eff}}}^{(2)}=-[(2{\chi_{15}}^{(2)}+{\chi_{31}}^{(2)})\cos^2\theta'+{\chi_{33}}^{(2)}\sin^2\theta']\sin\theta' \qquad (3b)$$

Configuration (3):

$${\chi_{\text{eff}}}^{(2)}=-{\chi_{15}}^{(2)}\sin\theta'=-{\chi_{15}}^{(2)}\frac{\sin\theta}{n_\omega} \qquad (3c)$$

The three non-zero components of the ${\chi_{ij}}^{(2)}$ $(2\omega;\omega,\omega)$ susceptibility tensor for poled PMMA films (symmetry $C_{\infty v}$) containing compounds **1** and **2** have been measured and are listed in Table 7. For compound **1** the component ${\chi_{31}}^{(2)}={\chi_{zzx}}^{(2)}$ is much higher than ${\chi_{33}}^{(2)}={\chi_{zzz}}^{(2)}$, indicating that its nonlinear polarization behavior strongly departs from that expected for films with linear one-dimensional molecules wherein ${\chi_{33}}^{(2)}=3{\chi_{31}}^{(2)}$.[31] The values for compound **2** are not so striking although ${\chi_{31}}^{(2)}$ is as large as ${\chi_{33}}^{(2)}$. The above behavior has been associated with a perpendicular component of the optical transition moment in relation to $\Delta\mu=\mu^{(1)}-\mu^{(0)}$, *i.e.* the difference between the permanent dipole moments of the excited $\mu^{(1)}$ and ground $\mu^{(0)}$ states.[32] Since the permanent moments of both ground and excited states would be directed along the donor–acceptor z axis, the transition moments should present a component perpendicular to that axis. The presence of the perpendicular component of μ^{01} has been shown to induce strong off-diagonal components of the β tensor[32–34] and large deviations from Kleinman's symmetry condition[35] ($\beta_{31}=\beta_{15}$) under near-resonance conditions. This breaking of Kleinman's condition should, then, also apply to the ${\chi_{ij}}^{(2)}$ measured in poled films. In fact, a clear deviation from this condition is observed in our ${\chi_{ij}}^{(2)}$ data. Moreover, the occurrence of μ^{01} perpendicular to $\Delta\mu$ appears to be consistent with the data for poling on optical absorption spectra previously described (Table 6). In summary, both absorption and SHG data suggest a strong perpendicular component of μ^{01} in relation to $\mu^{(0)}$, and therefore to the effective donor–acceptor axis.

On the other hand, all non-zero ${\chi_{ij}}^{(2)}$ values are much smaller than those measured for the related *para*-ferrocenyl molecule **2′**, also shown in Table 7. In other words, molecular bending strongly reduces the SHG response in accordance

Table 6 Fundamental and harmonic polarization configurations for the SHG experiments

Configuration	E_ω	$E_{2\omega}$
1	X	Y
2	Y	Y
3	45°	X

Table 7 Susceptibility values, molecular concentrations and film thicknesses of compounds **1** and **2** and the related derivative **2′**

Sample	N/ 10^{19} cm^{-3}	${\chi_{31}}^{(2)}$/ 10^{-9} esu	${\chi_{15}}^{(2)}$/ 10^{-9} esu	${\chi_{33}}^{(2)}$/ 10^{-9} esu	Thickness/ μm
1	15	1.4	−0.9	−0.5	1.6
2	10.5	0.4	−0.4	0.3	1.8
2′[a]	7.2	1.5	−0.4	0.3	1.5
[b]	6	6.6	−4.2	−2.4	1.4

[a]Ref. 13. [b][4-$O_2NC_6H_4CH$=CHC_6H_4-4′-(η^5-C_5H_4)Fe(η^5-C_5H_5)].[13]

with the results obtained at a molecular level for simpler organic compounds such as nitroaniline.[36]

It should be also remarked that $\chi_{ij}^{(2)}$ values for compound **1** are very small in comparison with those for the related molecule where ferrocenyl is in *para* position and the C=C bridging link is substituted for the N=N one.[13] Since it has been previously shown that the effect of this substitution is to induce a decrease in $\chi_{ij}^{(2)}$ it can be, then, confidently concluded that the ferrocenyl groups in the *para* position lead to a much higher SHG response than in the *ortho* position as also inferred for compound **2**.

Finally, by comparing the $\chi_{ij}^{(2)}$ values for compounds **1** and **2**, after normalization for the same molecular concentration, the nitro group behaves as a stronger acceptor than the [Mo(Cl)(Tp^{An})(NO)] fragment as expected and found for the related linear compounds.[13]

Concluding remarks

The data reported in this paper provide new information on the potentialities of organometallic systems for second-order NLO applications. The non-centrosymmetry of the crystal structure of compound **1** opens a possible route for the design of systems having SHG yield in the solid state. Although the susceptibilities have been reduced in comparison to those of the corresponding *para*-ferrocenyl compounds, the values are still significant.

Moreover, the off-diagonal components $\chi_{31}^{(2)}$ and $\chi_{15}^{(2)}$ for compounds **1** and **2** are comparable or superior to the diagonal element $\chi_{33}^{(2)}$, suggesting that the optical transition μ^{01} and the change in permanent dipole moment $\Delta\mu=\mu^{(1)}-\mu^{(0)}$ are tilted (non-parallel) to each other. This would also account for the breaking of Kleinman's symmetry, *i.e.* $\chi_{31}^{(2)}\neq\chi_{15}^{(2)}$. The occurrence of the perpendicular component of μ^{01} is consistent with the effect of poling on optical absorption spectra. From the latter data it has been inferred that the tilting angle between μ^{01} and $\mu^{(0)}$ increases in the *ortho*- in relation to the *para*-ferrocenyl compounds. The results obtained show the relevance of the molecular structure to the susceptibility tensor and the risk of using simple linear charge-transport models to describe the molecular hyperpolarizability.

Experimental

Materials

Commercial reagents were used as supplied. All reaction solvents were dried and degassed according to standard methods prior to use. The starting complex [Mo(Cl)$_2$(Tp^{An})(NO)] was obtained by the described method.[37] 5-Nitro-2-nitrosotoluene **D** (Scheme 1, step e) was prepared from 2-methyl-4-nitroaniline by oxidation with Caro's acid.[38]

All reactions were carried out under an atmosphere of dry oxygen-free dinitrogen, but the products were handled in air. Silica gel 60 (70–230 mesh) was used for all chromatographic separations.

Physical measurements

Elemental analyses were carried out by the Center for Elemental Microanalysis at the Complutense University. FAB mass spectra were obtained on a VG AutoSpec spectrometer, infrared spectra on a FTIR Nicolet Magna-550 spectrophotometer with samples as KBr discs or dichloromethane solutions in the 4000–350 cm^{-1} region.

The ^{1}H and ^{13}C NMR spectra were obtained on a Varian VXR-300 (299.88 and 75.40 MHz for ^{1}H and ^{13}C respectively) or Bruker AM-300 (300.13 and 75.43 MHz for ^{1}H and ^{13}C respectively) spectrophotometer of the NMR Service from solutions in $CDCl_3$. Chemical shifts δ are listed in parts per million relative to tetramethylsilane. The ^{1}H and ^{13}C chemical shifs are accurate to 0.01 and 0.1 ppm respectively; coupling constants are accurate to $\pm$0.3 Hz for ^{1}H NMR spectra. The full assignment of the proton resonances was made by proton homonuclear decoupling techniques using the latter spectrophotometer. The nomenclature of the atoms used is shown in Fig. 1.

Cyclic voltammetric measurements were carried out on an Autolab apparatus equipped with a PSTA10 potentiostat using a three-electrode cell with platinum wires as working and auxiliary electrodes and a Ag–AgCl electrode as a reference, with a solution (*ca.* 10^{-3} mol dm^{-3}) of the complex in dichloromethane containing [NBu$_4$][BF$_4$] (0.2 mol dm^{-3}) as the base electrolyte, using a scan rate of 200 mV s^{-1}. Values are referred to an Ag–AgCl electrode, but ferrocene was used as internal standard.

UV-VIS spectra were recorded on a Cary 5G spectrophotometer with solutions in dichloromethane.

Preparation of ordered thin films

Films were prepared from chlorobenzene solutions containing the host polymer PMMA and the organometallic compound. For all systems, the masses of these two species in the solution were in a ratio from 10 to 1, respectively. The concentrations of organometallic molecules in the films, determined from the optical absorption spectra, ranged from 10.5×10^{19} to 15×10^{19} cm^{-3}. The film thicknesses were between 0.6 and 2 μm as measured with a standard profilometer. Molecular ordering was achieved by corona poling with the following performance parameters: sample temperature 65 °C, poling voltage 6 kV and poling time 30 min.

Optical techniques

Optical absorption spectra for the spin-coated films were measured in the wavelength range 300–800 nm with an Hitachi U-3501 spectrophotometer. The $\chi_{ij}^{(2)}$ susceptibilities were determined by the Maker fringes technique[29,39,40] using an *x*-cut $LiNbO_3$ plate as a reference ($\chi_{33}^{(2)}=1.96\times10^{-7}$ esu). A Q-switched Nd-YAG laser (10 ns pulse duration and 10 Hz repetition rate) operating at 1.064 μm was used as a fundamental source. The second-harmonic light signal was detected with a photomultiplier, averaged with a boxcar integrator and stored in a computer.

Crystal structure determination

Crystal data for complex 1. $C_{24}H_{21}FeN_3O_2$, $M=439.29$, orthorhombic, space group $Pna2_1$, $a=28.599(3)$, $b=7.2572(7)$, $c=19.614(2)$ Å, $V=4070.9(7)$ Å^3, $Z=8$ (two independent molecules per unit cell), $D_c=1.434$ g cm^{-3}, μ(Mo-Kα)$=0.767$ mm^{-1}, $F(000)=1824$, $T=295$ K.

The crystals of complex **1** were dark red, fibrous and polysynthetically twinned. The best crystal of prismatic shape and dimensions $0.1\times0.02\times0.04$ mm was coated with epoxy resin and mounted on a Siemens Smart CCD diffractometer equipped with graphite monochromated Mo-Kα radiation ($\lambda=0.71073$ Å). Data were collected using the ω scan technique over a quadrant of the reciprocal space by a combination of three exposure sets. Each exposure for 20 s covered 0.3° in ω. Unit cell dimensions were determined by a least-squares fit of 60 reflections and with $I>20\sigma(I)$. Intensity data were measured up to $2\theta_{max}=46.60°$ (h, −31 to 10; k, −8 to 7; l, −6 to 21). Upon averaging the 7921 reflections, 3680 of which were uniquely measured ($R_{int}=0.0673$), 2916 with $I>2\sigma(I)$ were considered observed. The structure was solved by direct methods (SIR 92)[41] and Fourier difference techniques and refined by full-matrix least squares on F^2 (SHELXL 93).[42] Anisotropic thermal parameters were used in the last cycles of refinement for all non-hydrogen atoms. Hydrogen atoms were calculated and refined as riding on carbon atoms with a

common isotropic displacement parameter. Convergence of 542 variable parameters by least-squares refinement on F^2 for 2916 observed reflections was reached at $R=0.08$ and $wR=0.18$ with a goodness of fit of 1.10. The largest residual peak and hole in the final difference map were $+0.682$ and -0.357 e Å^{-3} respectively.

CCDC reference number 1145/137.

Preparation of the complexes

2-Ferrocenyl-5-methylnitrobenzene A (Scheme 1, steps a–c). Ferrocene (3.80 g, 20.4 mmol) was added to sulfuric acid (specific gravity 1.84, 25 cm^3). The resulting deep blue ferrocenium solution was stirred at room temperature for 2 h, then poured into ice–water (100 cm^3) and allowed to warm to room temperature with stirring for *ca.* 30 min (step a).

A solution of sodium nitrite (0.91 g, 13.2 mmol) in water (5 cm^3) at 0 °C was added dropwise with stirring to a solution of 4-methyl-2-nitroaniline (1.83 g, 12.0 mmol) in 1:1 water–hydrochloric acid (specific gravity 1.18, 10 cm^3). The mixture was stirred at 0 °C for 45 min to ensure the full diazotization (step b).

Copper powder (1 g) was added to the ferrocenium solution. Then, the diazonium solution was added dropwise with vigorous stirring. After 24 h of stirring the nitrogen effervescence ceased, and ascorbic acid (5 g) was added to reduce the unreacted ferrocenium to ferrocene (step c).

The product was extracted with dichloromethane (6×25 cm^3). The combined organic extracts were filtered through Celite, and the solvent eliminated. The dark solid was purified by column chromatography with an increasing proportion of dichloromethane in *n*-hexane as the eluent. The first yellow-orange fraction eluted with pure *n*-hexane gave rise upon evaporation to ferrocene, and the second one eluted with 50% dichloromethane–*n*-hexane yielded the desired compound as a deep red solid (1.68 g, 43%), [$O_2NC_6H_3(5\text{-}CH_3)$-2-($\eta^5$-$C_5H_4$)Fe($\eta^5$-$C_5H_5$)] (Found: C, 63.17; H, 4.67; N, 4.36. $C_{17}H_{15}FeNO_2$ requires C, 63.58; H, 4.71; N, 4.36%). IR (KBr, cm^{-1}): 1527 and 1363, $\nu(NO_2)$; 891, π(CH). FAB$^+$: m/z 321 (M^+), 291 ($M-NO$) and 275 ($M-NO_2{}^+$). ^{1}H NMR ($CDCl_3$, room temperature): δ 7.69, 7.33, 7.29 [d, $^3J(HH)=8.1$, 1 H; d, $^4J(HH)=1.5$, 1H; dd, $^3J(HH)=8.1$, $^4J(HH)=1.5$, 1H; C_6H_3]; 4.45, 4.33 [t, $^3J(HH)=1.8$, 2H; t, $^3J(HH)=1.8$ Hz, 2H; C_5H_4]; 4.09 (s, 5H; C_5H_5) and 2.38 (s, 3H; CH_3). ^{13}C NMR ($CDCl_3$, room temperature): δ 137.8, 136.9, 131.4, 129.3, 123.4, 113.9 (C_6H_3); 81.3, 69.0, 68.5 (C_5H_4); 69.7 (C_5H_5) and 20.7 (CH_3).

2-Ferrocenyl-5-methylaniline B (Scheme 1, step d). A mixture of compound **A** (1.22 g 3.8 mmol) and granulated tin (1.3 g) in 1:1 hydrochloric acid (specific gravity 1.18) ethanol (35 cm^3) was refluxed with continuous stirring for 2 h. The solution changed from red to orange, then it was cooled at room temperature and neutralized with 40% aqueous sodium hydroxide. Water (80 cm^3) and dichloromethane (80 cm^3) were added and the organic layer was separated. The aqueous layer was extracted with further dichloromethane (3×35 cm^3). The combined organic extracts were dried over sodium carbonate, filtered and evaporated to dryness to give the desired product as an orange oil, [$H_2NC_6H_3(5\text{-}CH_3)$-2-($\eta^5$-$C_5H_4$)Fe($\eta^5$-$C_5H_5$)]. IR ($CH_2Cl_2$, cm^{-1}): 3443 and 3346, $\nu(NH_2)$; 896, π(CH). ^{1}H NMR ($CDCl_3$, room temperature): δ 7.27, 6.61, 6.58 [d, $^3J(HH)=8.0$, 1H; d, $^3J(HH)=8.0$, 1H; s, 1H; C_6H_3]; 4.60, 4.35 [t, $^3J(HH)=1.8$, 2H; t, $^3J(HH)=1.8$ Hz, 2H; C_5H_4]; 4.22 (s, 5H; C_5H_5); 3.97 (br s, 2H; NH_2) and 2.31 (s, 3H; CH_3). ^{13}C NMR ($CDCl_3$, room temperature): δ 143.8, 137.2, 129.9, 119.1, 119.0, 116.2 (C_6H_3); 85.4, 68.1, 67.4 (C_5H_4); 68.8 (C_5H_5) and 21.0 (CH_3).

2′-Ferrocenyl-2,5′-dimethyl-4-nitroazobenzene 1 (Scheme 1, step f). A mixture of compound **B** (1.12 g, 3.84 mmol) and 5-nitro-2-nitrosotoluene **D** (0.77 g, 9.7 mmol) in glacial acetic acid (85 cm^3) was stirred at room temperature for 5 d, changing from orange to red and finally to black. Then water (100 cm^3) and dichloromethane (100 cm^3) were added and the organic layer was separated. The aqueous layer was extracted with more dichloromethane (4×25 cm^3). The organic extracts were combined, dried over sodium carbonate, filtered and finally evaporated to dryness to yield a black crude product. This was purified by column chomatography with 2% tetrahydrofuran–dichloromethane as the eluent. The major purple band was collected and yielded upon evaporation a deep purple solid (0.5 g, 30%). The analytical and spectroscopic data of this compound are given in Table 1.

4-Amino-2′-ferrocenyl-2,5′-dimethylazobenzene E (Scheme 1, step g). A solution of compound **1** (0.2 g, 0.46 mmol) and sodium sulfide hydrate (0.4 g) in ethanol (40 cm^3) was refluxed with stirring for 1 h, changing from deep purple to red. Then the solution was allowed to cool at room temperature and the solvent removed *in vacuo*. The crude product was purified by column chromatography with dichloromethane as the eluent. The major red band was collected and evaporated to dryness, giving rise to a deep red solid (0.1 g, 53%), [4-$H_2NC_6H_3(2\text{-}CH_3)${N=$NC_6H_3(5'\text{-}CH_3)$-2′-($\eta^5$-$C_5H_4$)Fe($\eta^5$-$C_5H_5$)}] Found: C, 66.92; H, 5.97; N, 10.01. $C_{24}H_{23}FeN_3$ requires C, 70.41; H, 5.67; N, 10.27%). IR (KBr, cm^{-1}): 3466 and 3369, $\nu(NH_2)$; 896, π(CH). ^{1}H NMR ($CDCl_3$, room temperature): δ 7.64, 7.30, 7.15 [d, $^3J(HH)=8.6$, 1 H; d, $^4J(HH)=2.2$, 1H; dd, $^3J(HH)=8.6$, $^4J(HH)=2.2$, 1H; C_6H_3]; 7.65, 6.57, 6.61 [d, $^3J(HH)=8.0$, 1H; dd, $^3J(HH)=8.0$, $^4J(HH)=1.4$, 1H; d, $^4J(HH)=1.4$, 1H; C_6H_3]; 4.78, 4.34 [t, $^3J(HH)=1.8$, 2H; t, $^3J(HH)=1.8$ Hz, 2H; C_5H_4]; 4.03 (s, 5H; C_5H_5); 4.00 (br s, 2H; NH_2); 2.73, 2.38 (s, 3H; s, 3H; CH_3). ^{13}C NMR ($CDCl_3$, room temperature): δ 150.6, 149.0, 144.0, 141.1, 136.0, 134.3, 129.7, 129.4, 117.6, 116.6, 115.8, 112.9 (C_6H_3); 83.2, 70.4, 68.6 (C_5H_4); 69.4 (C_5H_5); 21.1, 17.7 (CH_3).

[Mo(Cl)(Tp^{An})(NO){$NHC_6H_3(3\text{-}CH_3)$[N=$NC_6H_3(5\text{-}CH_3)$-2-(η^5-C_5H_4)Fe(η^5-C_5H_5)]-4}] 2 (Scheme 1, step h). A solution of compound **E** (0.06 g, 0.15 mmol), [$Mo(Cl)_2$(Tp^{An})(NO)] (0.105 g, 0.15 mmol) and triethylamine (0.15 mL, 1.09 mmol) was stirred under reflux in toluene (15 cm^3) for 5 h, changing from brownish red to deep purple. Then the reaction mixture was allowed to cool at room temperature and evaporated to dryness under reduced pressure. The resulting solid was purified by column chromatography on silica gel using 1% tetrahydrofuran–dichloromethane as the eluent. The major purple band was collected and evaporated, yielding a deep purple solid (0.13 g, 74%). The analytical and spectroscopic data of **2** are in Table 1.

Acknowledgements

We acknowledge financial support from projects PB95–0370, TIC 96–0668 and european contract CI1*-CT94–0039.

References

1 D. S. Chemla and J. Zyss, *Nonlinear Optical Properties of Molecules and Crystals*, Academic Press, New York, 1987.
2 P. N. Prasad and D. J. Williams, *Introduction to Nonlinear Optical Effects in Molecules and Polymers*, Wiley, New York, 1991.
3 J. Zyss (Editor), *Molecular Nonlinear Optics: Materials, Physics, Devices*, Academic Press, Boston, 1994.
4 C. Bosshard, K. Sutter, P. Prêtre, J. Hulliger, M. Flörsheimer, P. Kaatz and P. Günter, *Organic Nonlinear Optical Materials*, Gordon and Breach Science Publishers, Amsterdam, 1995.
5 S. R. Marder, J. E. Sohn and G. D. Stucky (Editors), *ACS Symp. Ser.*, 1991, **455**.
6 S. R. Marder and J. W. Perry, *Organic, Metallo-Organic and*

Polymeric Materials for Nonlinear Optical Applications, Proc. SPIE, The International Society for Optical Engineering, Washington, DC, 1994.
7 H. S. Nalwa and S. Miyata, *Nonlinear Optics of Organic Molecules and Polymers*, CRC Press, Boca Raton, FL, 1996.
8 M. L. Green, S. R. Marder, M. E. Thompson, J. A. Brandy, D. Bloor, P. V. Kolinsky and R. J. Jones, *Nature* (*London*), 1987, **330**, 360.
9 H. S. Nalwa, *Appl. Organomet. Chem.*, 1991, **5**, 349.
10 N. J. Long, *Angew. Chem.*, *Int. Ed. Engl.*, 1995, **34**, 21.
11 R.A. Hahn and D. Bloor (Editors), *Organic Materials for Nonlinear Optics*, Spec. Publ. No. 69, The Royal Society of Chemistry, London, 1989.
12 R.A. Hahn and D. Bloor (Editors), *Organic Materials for Nonlinear Optics II*, Spec. Publ. No. 91, The Royal Society of Chemistry, Cambridge, 1991.
13 C. López-Garabito, J. A. Campo, J. V. Heras, M. Cano, G. Rojo and F. Agulló-López, *J. Phys. Chem. B*, 1998, **102**, 10698.
14 R. B. Comizzoli, *J. Electrochem. Soc.: Solid State Technol.*, 1987, **134**, 424.
15 B. J. Coe, C. J. Jones, J. A. McCleverty, D. Bloor and G. H. Cross, *J. Organomet. Chem.,* 1994, **464**, 225.
16 M. Rosemblum, *Chemistry of the Iron Group Metallocenes*, Wiley, New York, 1965.
17 B. J. Coe, T. A. Hamor, C. J. Jones, J. A. McCleverty, D. Bloor, G. H. Cross and T. L. Axon, *J. Chem. Soc.*, *Dalton Trans.*, 1995, 673.
18 B. J. Coe, C. J. Jones, J. A. McCleverty, D. Bloor, P. V. Kolinsky and R. J. Jones, *Polyhedron,* 1994, **13**, 2107.
19 B. J. Coe, J. D. Foulon, T. A. Hamor, C. J. Jones, J. A. McCleverty, D. Bloor, G. H. Cross and T. L. Axon, *J. Chem. Soc.*, *Dalton Trans.*, 1994, 3427.
20 M. Nardelli, *J. Appl. Crystallogr.*, 1995, **28**, 659.
21 C. K. Johnson, ORTEP, Report ORNL-5138, Oak Ridge National Laboratory, Oak Ridge, TN, 1976.
22 B. J. Coe, J. D. Foulon, T. A. Hamor, C. J. Jones and J. A. McCleverty, *Acta Crystallogr.*, *Sect. C*, 1991, **47**, 2032.
23 A. Togni and G. Rihs, *Organometallics*, 1993, **12**, 3368.
24 F. H. Allen, O. Kennard, D. G. Watson, L. Brammer, A. G. Orpen and R. Taylor, *J. Chem. Soc.*, *Perkin Trans. 2*, 1987, S1.
25 A. G. Orpen, L. Brammer, F. H. Allen, O. Kennard, D. G. Watson and R. Taylor, *J. Chem. Soc.*, *Dalton Trans.*, 1989, S1.
26 E. C. Constable, A. J. Edwards, R. Martínez-Máñez and P. R. Raithby, *J. Chem. Soc.*, *Dalton Trans.*, 1995, 3253; M. E. N. P. R. A. Silva, A. J. L. Pombeiro, J. J. R. Frausto da Silva, R. Hermann, N. Deus, T. J. Castilho and R. E. Bozak, *J. Organomet. Chem.*, 1994, **480**, 81.
27 M. A. Mortazavi, A. Knoesen, S. T. Towel, B. G. Higgings and A. Dienes, *J. Opt. Soc. Am.*, 1989, **B6**, 733.
28 D. R. Martínez, K. Koch, F. K. Ratsorong and G. O. Carlinge, *J. Appl. Phys.*, 1994, **75**, 4273.
29 J. Zyss and D. S. Chemla, in *Nonlinear Optical Properties of Molecules and Crystals*, Academic Press, Orlando, FL, 1987, vol. 1, p. 23.
30 L. M. Hayden, G. F. Sauter, F. R. Ore, P. L. Pasillas, J. M. Hoover, G. A. Lindsay and R. A. Henry, *J. Appl. Phys.*, 1990, **68**, 456.
31 K. D. Singer, M. G. Kuzyk, W. R. Holland, J. E. Sohn, S. J. Lalama, R. B. Comizzoli, H. E. Katz and M. L. Schilling, *Appl. Phys. Lett.*, 1988, **53**, 1800.
32 R. Wortmann, P. Krämer, C. Glania, S. Lebus and N. Detzer, *Chem. Phys.*, 1992, **173**, 99.
33 J. J. Wolf, D. Langle, D. Hillenbrand, R. Wortmann, R. Matschiner, C. Glania and P. Krämer, *Adv. Mater*., 1997, **9**, 138.
34 H. S. Nalwa, T. Watanabe and S. Miyata, *Adv. Mater*., 1995, **7**, 754.
35 S. F. Hubbard, R. G. Petschek, K. D. Singer, N. D'Sidocky, C. Hudson, K. D. Chien, C. C. Henderson and P. A. Cahill, *J. Opt. Soc. Am.*, 1998, **B15**, 289.
36 J. L. Oudar and D. S. Chemla, *J. Phys. Chem.,* 1977, **66**, 2664.
37 M. Cano, J. V. Heras, A. Monge, E. Gutiérrez, C. J. Jones, S. L. W. McWhinnie and J. A. McCleverty, *J. Chem. Soc.*, *Dalton Trans.*, 1992, 2435.
38 W. P. Langley, *Org. Synth.*, 1955, Coll. Vol. III, 334.
39 M. Eich, A. Sen, H. Looser, G. C. Bjorklund, J. D. Swalen, R. Tweig and D. Y. Yoon, *J. Appl. Phys.*, 1989, **66**, 2559.
40 G. Rojo, A. Hierro, M. A. Diaz-García, F. Agulló-López, B. del Rey, A. Sastre and T. Torres, *Appl. Phys. Lett.*, 1997, **70**, 1802.
41 A. Altomare, G. Cascarano, C. Giacovazzo and A. Guagliardi, *J. Appl. Crystallogr.*, 1994, **27**, 435.
42 G. M. Sheldrick, SHELXL 93, University of Göttingen, 1993.

Paper 8/08936A